

Published in final edited form as:

Prostaglandins Other Lipid Mediat. 2014 October ; 0: 52–61. doi:10.1016/j.prostaglandins.2014.08.003.

LYSOPHOSPHOLIPID ACYLTRANSFERASES AND EICOSANOID BIOSYNTHESIS IN ZEBRAFISH MYELOID CELLS

Simona Zarini, Joseph A. Hankin, Robert C. Murphy, and Miguel A. Gijón

Department of Pharmacology, University of Colorado Denver, Aurora, CO 80045

Abstract

Eicosanoids derived from the enzymatic oxidation of arachidonic acid play important roles in a large number of physiological and pathological processes in humans. Many animal and cellular models have been used to investigate the intricate mechanisms regulating their biosynthesis and actions. Zebrafish is a widely used model to study the embryonic development of vertebrates. It expresses homologs of the key enzymes involved in eicosanoid production, and eicosanoids have been detected in extracts from adult or embryonic fish. In this study we prepared cell suspensions from kidney marrow, the main hematopoietic organ in fish. Upon stimulation with calcium ionophore, these cells produced eicosanoids including PGE₂, LTB₄, 5-HETE and, most abundantly, 12-HETE. They also produced small amounts of LTB₅ derived from eicosapentaenoic acid. These eicosanoids were also produced in kidney marrow cells stimulated with ATP, and this production was greatly enhanced by preincubation with thimerosal, an inhibitor of arachidonate reacylation into phospholipids. Microsomes from these cells exhibited acyltransferase activities consistent with expression of MBOAT5/LPCAT3 and MBOAT7/LPIAT1, the main arachidonoyl-CoA:lysophospholipid acyltransferases. In summary, this work introduces a new cellular model to study the regulation of eicosanoid production through a phospholipid deacylation-reacylation cycle from a well-established, versatile vertebrate model species.

Keywords

arachidonic acid; eicosanoids; prostaglandins; leukotrienes; lipid mediators of inflammation; animal models; zebrafish; lysophospholipid acyltransferases; phospholipids

1. Introduction

Eicosanoids are a wide family of molecules that derive from the oxidation of arachidonic acid (AA) through a variety of metabolic pathways. Many eicosanoids are mediators that act in an autocrine or paracrine fashion to trigger proinflammatory, or in some cases anti-

© 2014 Elsevier Inc. All rights reserved.

Corresponding author: Miguel A. Gijón, Ph.D., 12801 E. 17th Ave., L18-6119, Aurora, CO 80045, Tel: (303) 724-3353, Fax: (303) 724-3357, miguel.gijon@ucdenver.edu.

Publisher's Disclaimer: This is a PDF file of an unedited manuscript that has been accepted for publication. As a service to our customers we are providing this early version of the manuscript. The manuscript will undergo copyediting, typesetting, and review of the resulting proof before it is published in its final citable form. Please note that during the production process errors may be discovered which could affect the content, and all legal disclaimers that apply to the journal pertain.

inflammatory responses in cells and tissues [1–3]. Biosynthesis of eicosanoids is tightly regulated in cells, and has been extensively investigated for many decades since the elucidation of the chemical structures of prostaglandins (PGs) and leukotrienes (LTs) [4,5]. One of the key factors regulating eicosanoid production is the cellular level of free AA, controlled to a great extent by a deacylation-reacylation biochemical cycle known as the Lands cycle [6]. Considerable effort has been dedicated to investigating the release of AA from membrane phospholipids by the action of phospholipases A₂, particularly by cytosolic phospholipase A₂ alpha (cPLA₂α, also known as Group IVA PLA₂) [7]. There is also evidence of AA release in some models through the action of monoacylglycerol lipase on AA-containing diglycerides [8]. However, much less is known about the role of reacylation of AA into phospholipids or triglycerides in controlling the levels of free AA and eicosanoid production. This is primarily due to the fact that many of the key enzymes implicated have not been identified until relatively recently, particularly lysophospholipid acyltransferases (LPATs) [9–14]. Some groups, including ours, have now linked two of the LPATs, namely MBOAT5 (also known as LPCAT3) and MBOAT7 (also known as LPIAT1) with regulating AA release and eicosanoid production in human neutrophils and human monocytes [15,16], but not much is known about the potential role of other LPATs or other experimental models.

Despite a sizable body of scientific literature on this subject, there are still many areas that are not well understood about eicosanoid production, and new models of study could prove helpful in providing new insight into their regulation and possible pharmacological targets. Zebrafish (*Danio rerio*) is a unique model in the study of the embryonic development of vertebrates. This animal model is also very prolific, comparatively inexpensive to maintain and amenable to genetic manipulation with a much shorter time frame than other widely used animal models, such as rodents. Like most fish, zebrafish contain abundant n-3 fatty acids such as eicosapentaenoic (EPA, 20:5) and docosahexaenoic (DHA, 22:6), probably due to a big extent to the composition of their diet [17]. However, they also contain AA (20:4 n-6), and AA-derived eicosanoids such as PGs have been observed in whole fish homogenates, where their levels are decreased by pretreatment with cyclooxygenase (COX) inhibitors [18]. In addition, a number of models of inflammation, both local and systemic [19–21], are available in the zebrafish and all of the relevant enzymes that are known to be involved in the Lands cycle in mammals have homologs in zebrafish [22] (also searchable at zfin.org). These enzymes include a number of phospholipases A₂ including cPLA₂α, acyl-CoA synthases and LPATs including MBOAT5 and MBOAT7. All of these factors make zebrafish an interesting model to study the regulation of eicosanoid production, although there are still some areas where little information is available. For instance, the possible cellular sources of free AA and eicosanoids are not known. Although fish are enriched in polyunsaturated fatty acyl chains, no detailed analysis of the intact phospholipid molecular species that contain esterified arachidonate in the zebrafish has been published. More importantly, a cellular model derived from the zebrafish that would permit facile analysis of different pro-inflammatory stimuli, chemical inhibitors or genetic manipulation and their effect on eicosanoid production is currently not available. The main goal of this research is to present such a cellular model.

Myeloid cells in general, and neutrophils in particular, have been very useful in studying eicosanoid production, since they readily synthesize eicosanoids when challenged with a variety of stimuli. Using the non-specific inhibitor thimerosal, our group showed that inhibition of MBOAT5 and MBOAT7 results in a remarkable increase in the synthesis of leukotriene B₄ (LTB₄) by human neutrophils stimulated by the combination of granulocyte-macrophage colony-stimulating factor (GM-CSF) and formyl-methionyl-leucyl-phenylalanine (fMLP) [23]. Unfortunately, it is not feasible to obtain sufficient numbers of peripheral blood neutrophils from zebrafish. We have previously shown that myeloid cells from the mouse bone marrow cells are able to produce abundant LTB₄ when stimulated by fMLP or zymosan [24]. The functional equivalent of the mammalian bone marrow, the anatomical site of the production of myeloid cells destined to circulate in the blood of zebrafish, is the kidney marrow [25]. Kidney marrow cells from zebrafish were isolated and evaluated as a possible model for eicosanoid production and acyltransferase activity.

2. Materials and methods

2.1. Reagents

Salts, HPLC-grade solvents, calcium ionophore A23187, and dihydroxyacetophenone (DHAP) were purchased from Fisher Scientific (Pittsburgh, PA). Bovine serum albumin (BSA), ATP, and thimerosal were purchased from Sigma–Aldrich (St. Louis, MO). Lysophospholipids, fatty acyl-CoA esters and deuterated phospholipid internal standards were obtained from Avanti Polar Lipids (Alabaster, AL). Protease inhibitor cocktail tablets were obtained from Roche Molecular Diagnostics GmbH (Mannheim, Germany). Standard and stable isotope-labeled eicosanoids were purchased from Cayman Chemical Co. (Ann Arbor, MI).

2.2. Zebrafish kidney dissection and kidney marrow cell isolation

Adult and larval (3 dpf) zebrafish were obtained from the zebrafish facility at the University of Colorado Center for Comparative Medicine. They were maintained at 28.5 °C with a light/dark cycle of 10/14 h according to established procedures [26]. All procedures were performed following guidelines approved by the Institutional Animal Care and Use Committee at the University of Colorado Denver. Kidneys were dissected from adult fish and kidney marrow cells isolated according to Le Blanc *et al.* [27], with minor modifications. Briefly, after euthanizing the zebrafish by submersion in iced water, kidneys from 20–25 zebrafish were isolated into 10 mL of 0.9X PBS supplemented with 5 % FCS and 1 % penicillin/streptomycin solution. The kidneys were then broken apart using first a 1 mL pipet and then a 10 mL syringe with an 18G needle. After centrifuging at 500 × *g* for 8 min, the pellet was resuspended and filtered through a 40-µm cell strainer. The filtrate was centrifuged and the kidney marrow cells resuspended in Hanks Balanced Salt Solution without calcium, magnesium or phenol red (HBSS[−]). The cellular distribution was verified by cytospin on microscopy slides and staining using a Hema 3 Stain Set (Fisher Scientific), following the manufacturer's instructions. Identification of the different cell types was carried out by comparison with published cytological data [25].

2.3. Lysophospholipid acyltransferase activity assay

Microsomes from zebrafish kidney marrow cells were prepared by resuspending the cells in homogenization buffer (250 mM sucrose, 50 mM Tris/HCl, pH 7.4, 1 mM EDTA, 20 % glycerol, and protease inhibitor cocktail) and disrupting them by sonication. The homogenate was centrifuged at $15,000 \times g$ for 15 min at 4 °C to pellet unbroken cells and nuclei. The supernatant was then centrifuged at $100,000 \times g$ for 1 h at 4 °C and the microsome pellet was resuspended in assay buffer (150 mM NaCl, 10 mM Tris/HCl, pH 7.4, 1 mM EDTA). Protein content was determined by the bicinchoninic acid assay (Pierce, Rockford, IL), using BSA as standard.

Zebrafish kidney marrow cell microsomes were tested for acyltransferase activity as described by Martin *et al.* [28]. Microsomes (10 µg protein) were incubated with 3 µM each of eight acyl-CoAs (14:0, 16:0, 18:0, 18:1, 18:2, 20:4, 20:5, and 22:6), 3 µM each of six lysophospholipids (LPA, LPC, LPE, LPG, LPI, and LPS), and 12.5 µM BSA, in the presence or absence of thimerosal (50 µM). The reaction was allowed to proceed for 10 min at 37 °C. Reaction was stopped by addition of 500 µL of methanol, prior to phospholipid extraction.

2.4. Phospholipid extraction and liquid chromatography/mass spectrometry

After addition of the deuterated internal standards [$^2\text{H}_3$]16:0/18:1-PA, [$^2\text{H}_3$]16:0/18:1-PC, [$^2\text{H}_3$]16:0/18:1-PE, [$^2\text{H}_3$]16:0/18:1-PG, [$^2\text{H}_3$]16:0/18:1-PI and [$^2\text{H}_3$]16:0/18:1-PS (25 ng each), samples were extracted according to the method of Bligh and Dyer [29]. The organic phase was dried under a stream of nitrogen gas and resuspended in 100 µL of a mixture of 75 % HPLC solvent C (hexanes/isopropanol 30:40, v/v) and 25 % solvent D (5 mM ammonium acetate in hexanes/isopropanol/water 30:40:7, v/v/v). Samples were injected into an HPLC system connected to a triple quadrupole mass spectrometer (API3200, AB SCIEX, Framingham, MA) and normal phase chromatography was performed using a silica HPLC column (Ascentis, 150 × 2.1 mm, 5 µm, Supelco, Bellefonte, PA) at a flow rate of 200 µL/min. Solvent D was maintained at 25 % for 5 min, increased gradually to 60 % in 10 min and then to 95 % in 5 min, and was held for 20 min before re-equilibration for 15 min. Mass spectrometric analysis was performed in the negative ion mode using multiple-reaction monitoring (MRM) of the forty-eight molecular species potentially generated during the enzymatic assay, plus the six deuterated standards [28]. The precursor ions monitored were the molecular ions $[\text{M}-\text{H}]^-$, except for PC in which case the acetate adducts $[\text{M}+\text{CH}_3\text{COO}]^-$ were monitored. The product ions analyzed after collision-induced decomposition were the carboxylate anions corresponding to the acyl chains. Results are reported as the ratio between the integrated area of each analyte and the integrated area of the corresponding internal standard for each class.

Endogenous phospholipids from zebrafish kidney marrow cell microsomes (10 µg protein) were extracted and analyzed as described above, except that LC-MS/MS analysis was performed using scheduled MRM to detect molecular species containing combinations of common fatty acyl chains [30]. Additionally, phospholipids containing esterified AA chains were analyzed by scanning precursor ions of the m/z 303 product anion. Since no standard dilution curves were used, these results cannot be used to quantitate absolute amounts of the

analytes, but they are useful to identify potential changes within each phospholipid class between different samples.

2.5. MALDI IMS of zebrafish larvae

Zebrafish larvae (3 dpf) were euthanized and manually placed into a shallow bed of modified optimal cutting-temperature compound to assist in cutting slices for MALDI imaging [31]. Slices (10- μm thick) were carefully collected onto glass coverslips, desiccated for 10 min at 25 Torr, and attached to a steel MALDI plate using copper tape. Matrix (DHAP) was applied by sublimation [31]. Data were acquired on a QStar XL hybrid quadrupole/quadrupole/TOF mass spectrometer (Applied Biosystems/MDS Sciex, currently AB SCIEX) using solid state laser at a pulse rate of 1000 Hz, 8.4 μJ laser power, and 50 μm \times 50 μm pixel size. Mass spectrometer parameters included declustering potential of -20 V, focusing potential of -30 V, and mass range of 400–1000 Da. Image data files were processed from “.RAW” format to “.IMG” format at a mass resolution of 0.1 Da using a software script supplied by Applied Biosystems. Data were viewed as two-dimensional displays of intensity per specific m/z value using TissueView software package from AB SCIEX.

2.6. Cell stimulation and eicosanoid extraction

Kidney marrow cells were suspended in HBSS⁼ at the concentration of 1×10^6 cells/mL and, after addition of CaCl_2 (2 mM) and MgCl_2 (0.5 mM), stimulated at 28.5 °C with calcium ionophore A23187 (0.5 μM , 15 min) or ATP (0.1 mM, 15 min). Before stimulation with ATP, cells were pretreated for 5 min with thimerosal (25 μM) or vehicle (HBSS⁼). Reactions were terminated by addition of 1 mL methanol. After addition of the internal standards [$^2\text{H}_4$]LTB₄, [$^2\text{H}_5$]LTD₄, [$^2\text{H}_8$]5-HETE, [$^2\text{H}_4$]PGF_{2 α} , [$^2\text{H}_4$]PGE₂, [$^2\text{H}_4$]PGD₂, [$^2\text{H}_4$]TXB₂ (2 ng each), [$^2\text{H}_5$]LTC₄, [$^2\text{H}_5$]LTE₄ and [$^2\text{H}_4$]6-keto-PGF_{1 α} (5 ng each), and [$^2\text{H}_8$]AA, (10 ng), the samples were centrifuged and supernatants diluted with water to a final methanol concentration of less than 15 % (v/v) and extracted using Strata-X 33u polymeric reverse phase cartridges (60 mg/1 mL, Phenomenex, Torrance, CA) preconditioned with 1 mL methanol and 1 mL water. The eluate (in 1 mL methanol) was dried down and resuspended in a mixture of 40 μL HPLC solvent A (8.3 mM acetic acid buffered to pH 5.7 with ammonium hydroxide) and 20 μL solvent B (acetonitrile/methanol, 65/35, v/v).

2.7. Metabolite separation and analysis by reverse-phase HPLC coupled to electrospray ionization mass spectrometry (LC-MS/MS)

An aliquot of each sample (20 μL) was injected into a HPLC column (Accucore C18 50 \times 3 mm, 2.6 μm , Thermo Scientific, Waltham, MA) and eluted at a flow rate of 300 $\mu\text{L}/\text{min}$ with a linear gradient of HPLC solvent B, which was increased from 45 % to 75 % in 6.5 min, to 98 % in 1 min, and held at 98 % for a further 6.5 min before re-equilibration at 45 % for 10 min. The HPLC system was directly interfaced into the electrospray source of a triple quadrupole mass spectrometer (API 3000, PE-Sciex, currently AB SCIEX) where mass spectrometric analysis was performed in the negative ion mode using MRM of the following specific m/z transitions (precursor ion \rightarrow product ion): 351 \rightarrow 233, PGD₂; 351 \rightarrow 271,

PGE₂; 349 → 189, PGE₃; 369 → 163, 6-keto-PGF_{1α}; 353 → 193, PGF_{2α}; 333 → 189, PGA₂ and PGJ₂; 315 → 203, 15-deoxy-PGJ₂; 369 → 169, TXB₂; 367 → 169, TXB₃; 351 → 217, LXA₄; 351 → 221, LXB₄; 335 → 195, LTB₄, ⁶-*trans*-LTB_{4s} and 5,12-diHETEs; 351 → 195, 20-OH-LTB₄; 365 → 195, 20-COOH-LTB₄; 335 → 115, 5,6-diHETEs; 333 → 195, LTB₅; 624 → 272, LTC₄; 495 → 177, LTD₄; 438 → 333, LTE₄; 319 → 115, 5-HETE; 317 → 203, 5-oxo-EETE; 319 → 179, 12-HETE; 319 → 219, 15-HETE; 343 → 245 and 343 → 273, 17-OH-DHA; 319 → 191, 5,6-EET; 319 → 155, 8,9-EET; 319 → 167, 11,12-EET; 319 → 113, 14,15-EET; 303 → 205, AA; 327 → 283, DHA; 301 → 203, EPA; 355 → 237, [²H₄]PGD₂; 355 → 275, [²H₄]PGE₂; 373 → 167, [²H₄]6-keto-PGF_{1α}; 357 → 197, [²H₄]PGF_{2α}; 373 → 173, [²H₄]TXB₂; 339 → 197, [²H₄]LTB₄; 629 → 272, [²H₅]LTC₄; 500 → 177, [²H₅]LTD₄; 443 → 338, [²H₅]LTE₄; 327 → 116, [²H₈]5-HETE; and 311 → 267, [²H₈]AA. Quantitation was performed using standard isotope dilution as previously described [32].

3. Results

3.1. Arachidonoyl-containing phosphatidylethanolamines in the zebrafish kidney

A major goal of this study was to establish a reliable cellular model derived from the zebrafish that would permit studies on the regulation of eicosanoid biosynthesis. We have previously used mouse bone marrow cells, both as a mixed population and as purified neutrophils, and found them to be a useful model of prostaglandin and leukotriene production when challenged with different stimuli [24]. Based on that fact, we decided to test the zebrafish functional equivalent of the mammalian bone marrow, which is the kidney marrow, the source of blood cells in the zebrafish [25]. There is very little information in the scientific literature about intact molecular species of phospholipids that contain esterified arachidonate. Whole kidneys from adult zebrafish were dissected, and lipids were extracted following the method of Bligh and Dyer [29]. Phospholipids classes were then separated by normal-phase HPLC and analyzed using two different mass spectrometry-based approaches. LC-MS analysis of all negative ions between *m/z* 250 and 1650 revealed a complex mixture of phospholipids across the different classes. As an example, analysis of the negative molecular ions, [M-H]⁻, eluting at the retention time of a deuterated PE internal standard showed numerous PE molecular species, including several that contained multiple double bonds (Fig. 1). The measured mass information alone is not sufficient to assign fatty acyl chain composition, so this analysis was complemented by LC-MS/MS analysis in the MRM mode, based on collision-induced decomposition of the molecular negative ions to yield the carboxylate anions corresponding to the acyl chains. It is important to note that no positional information was gleaned from this type of experiment, as indicated by the use of an underscore character between the acyl chains [33]. Although preliminary experiments with synthetic standards showed some differences in intensities of the anions from the *sn*-1 or *sn*-2 positions of phospholipids, these differences were not sufficient to determine unequivocally the position where these acyl chains were in the intact molecule. Also, these experiments offered no information about the position or the configuration of the double bonds. However, these data revealed that PEs in the zebrafish kidney were enriched in molecular species containing polyunsaturated acyl chains, including 22:6, 20:5 and 20:4. Interestingly, some of the 20:4-containing PE molecular species, such as 16:0_20:4-PE,

when analyzed by imaging mass spectrometry of zebrafish larvae appeared to be particularly enriched in an area that, according to anatomical atlases (zfin.org), corresponded approximately to the location of the pleuroperitoneal cavity containing the gut, the liver and the embryonic kidney (inset of Fig. 1). Therefore, both in larval and adult zebrafish, potential precursor pools of AA were abundant in the anatomical area where blood cells are produced. As shown later, 20:4-containing molecular species were also rather abundant in the other phospholipid classes analyzed.

3.2. Isolation of zebrafish kidney marrow cells and eicosanoid production upon calcium ionophore treatment

We followed a previously published protocol to isolate kidney marrow cells from dissected zebrafish kidneys [27]. The resulting cellular suspension was analyzed by cyto-spin on microscopy slides and cell staining. It consistently showed a cellular population very similar to that previously published, with a very abundant presence of myeloid cells, including two lineages of granulocytes: neutrophils and basophils/eosinophils [25]. We evaluated the ability of these cells to synthesize eicosanoids after stimulation with calcium ionophore A23187, an ion carrier molecule that selectively renders membranes permeable to calcium ions and increases their level in the cytosol. A23187 is a trigger of AA and eicosanoid release from many cells, including human peripheral blood neutrophils and mouse bone marrow cells [23,24]. LC-MS/MS was used to detect eicosanoids derived from the oxidation of AA, as well as the free fatty acids AA, EPA and DHA. A representative chromatogram showing the intensities of the $[M-H]^-$ ions derived from several lipids from A23187-stimulated kidney marrow cells is presented in Fig. 2 (bottom panel). A variety of eicosanoids was generated from AA both through the COX pathway, like PGE₂, and through the 5-lipoxygenase (5-LO) pathway, including 5-HETE, LTB₄ and its ω -oxidized metabolite 20-OH-LTB₄, together with the non-enzymatic LTA₄ derivatives ⁶-*trans*-LTB₄ and 5,6-diHETE isomers. Leukotriene B₅ (LTB₅), derived from the action of 5-LO on EPA, was also detected. Interestingly, the most abundant eicosanoid synthesized by these cells after stimulation with calcium ionophore was 12-HETE, a product of the action of 12-lipoxygenase (12-LO). Modest levels of 5,12-diHETE isomers, very likely synthesized by the action of 12-LO on 5-HETE, were also observed in these cells. Despite the abundance of DHA, no 17-OH-DHA, which is a precursor of resolvin D1, was detected in this short-term stimulation. In view of the suggestion for robust 12-LO activity, we also tested some extracts of A23187-stimulated kidney marrow cells for the presence of 14-OH-DHA by adding the transition m/z 343→281 [34], but no signal was detected. Free EPA, DHA, and AA were the only lipids detected in unstimulated, control cells (top panel), but only AA increased after stimulation with A23187.

3.3. Effect of thimerosal on eicosanoid synthesis by kidney marrow cells stimulated with ATP

Thimerosal, which inhibits AA reacylation into phospholipids, was examined as an agent that could exert an effect on eicosanoid synthesis in zebrafish kidney marrow cells stimulated with ATP, a physiological stimulus that increases cytosolic calcium via interaction with specific P₂-type purinergic receptors [35]. When cells were stimulated with ATP alone, only small increases in PGE₂, 5-HETE and 12-HETE levels were observed

compared to control untreated cells (Fig. 3). The signal for LTB₄ was below the detection limit in control and ATP-stimulated cells. When cells were treated with thimerosal, but without ATP, no increase in eicosanoids compared to control samples was observed. However, preincubation with thimerosal followed by ATP stimulation resulted in a dramatic increase in the synthesis of PGE₂, LTB₄, 5-HETE, and 12-HETE. These results suggested a synergistic effect between ATP, most likely through activation of cPLA₂ α , and thimerosal, probably through inhibition of AA reacylation, similar to what was previously observed in human neutrophils [23].

3.4. Phospholipid analysis of microsomes from zebrafish kidney marrow cells

The major arachidonoyl:lysophospholipid reacylating enzymes, MBOAT5 and MBOAT7, are predicted to be integral membrane proteins, and their activities are readily measured in microsomal preparations [15,28]. Initially, the endogenous phospholipids present in microsomes from zebrafish myeloid cells were examined using two different LC-MS/MS strategies. Microsomes were prepared from isolated kidney marrow cells after filtering out the kidney tubules. Therefore, the results represent a more detailed report of the phospholipid molecular species that make up the membranes of zebrafish kidney marrow cells, compared with the whole kidney extract used for the data presented in Fig. 1. We first analyzed, using normal-phase HPLC and MRM in the negative-ion mode, all possible combinations of the more common acyl chains (Table 1). Because of different ionization efficiencies of each phospholipid class and the impracticability of constructing calibration curves for every molecular species detected, these results were not quantitative, and are presented as the percentage of each individual species compared with the most abundant one within the class, which is assigned the darkest tone for each color scale. Entries in white indicated molecular species that fell below the limit of detection under the conditions used for analysis. A wide variety of molecular species of phospholipids of every class was detected. There were numerous distinct PC molecular species, many of them at relatively low levels. In contrast, a comparatively small number of different PG molecular species was detected, although with quite robust signals. In the PI class, the 18:0_20:4 molecular species was much more abundant than any other. As shown for the PEs in the whole kidney (Fig. 1), it is worth noting the abundance of molecular species that contain polyunsaturated acyl chains. In fact, for PA and PS the most abundant species contained a 22:6 chain, whereas for PE and PI the most abundant species contained 20:4. As expected, the PC and particularly the PE classes contained abundant ether-linked molecular species, but some alkyl chains were also detected in the PG, PI and PS classes.

Molecular species containing 20:4 were found in all six phospholipid classes studied, making them potential precursor pools for AA release and eicosanoid production. Although the MRM analysis was quite comprehensive, we could not completely rule out the possibility that unexpected molecular species not included in the MRM list may be present in zebrafish kidney marrow cells. To investigate this, an alternative analysis was performed on the microsomal extracts, using LC-MS/MS to scan for negative precursor ions of the 20:4 carboxylate anion at m/z 303 [36]. This analysis is shown in Fig. 4. All the major ions that yielded m/z 303 fragment ions corresponded quite well to molecular species shown in Table 1, indicating that most, if not all, abundant phospholipid pools of AA in these cells were

represented in that table. Since phospholipids of each class have unique ionization efficiencies, it is not particularly meaningful to compare the intensities of the different lipids across classes. For instance, in aqueous solvents at neutral pH, PIs are found as anionic species and show corresponding strong signals for the molecular deprotonated ion upon electrospray ionization, whereas PCs, which are zwitterionic in aqueous solvents at neutral pH, generate weaker signals upon electrospray ionization as negative ions, resulting from adducts with the acetate present in the HPLC solvent system.

3.5. Acyltransferase activities on microsomes from zebrafish kidney marrow cells

The acyltransferase activities of zebrafish kidney cell microsomes were evaluated in a competitive assay using equimolar amounts of six 17:1-lysophospholipids (LPA, LPC, LPE, LPG, LPI and LPS), and of eight CoA esters (14:0, 16:0, 18:0, 18:1, 18:2, 20:4, 20:5 and 22:6). The assay was performed in the absence or presence of thimerosal, and was evaluated by analyzing the possible products of the reaction by LC-MS/MS in the MRM mode. The arachidonyl-CoA:lysophospholipid acyltransferase activities in this preparation are presented as the area ratio of the integrated area corresponding to each one of the MRM signals from newly synthesized 17:1/20:4 phospholipid divided by the integrated area of the deuterated internal standard in each class (Fig. 5). There was detectable AA reacylating activity for each of the classes, albeit to different extents. The highest activities were detected for PI and PC, followed by PE and PS. All these activities were substantially inhibited by thimerosal, indicating similarity between the AA-CoA:lysophospholipid acyltransferase activities in zebrafish kidney marrow cells and human neutrophils. This inhibitory effect by thimerosal was also consistent with the hypothesis that acyltransferase inhibition would result in increased free AA levels, and therefore enhanced eicosanoid production, as shown in Fig. 3.

The complete results of the acyltransferase activity assay on kidney marrow cell microsomes (Table 2) revealed a striking 20:4 reacylation capacity that was the highest activity for every class except for PS, where similar levels of activity using 20:4 or 20:5 chains were observed.

4. Discussion

The zebrafish has emerged as a valid model for several areas of research, including human disease [37,38], inflammation [19,21], neutrophil biology [19,39] and lipid metabolism [40]. Zebrafish has been shown to synthesize eicosanoids from exogenous precursors such as AA or PGH₂ [41,42], but endogenous eicosanoids have also been found in homogenates from these animals, including PGE₂, LTB₄, LXA₄, 5-HETE and 12-HETE [18,43,44]. PGE₂ levels in zebrafish extracts are decreased by treatment with indomethacin, a non-selective COX inhibitor, or with NS-398, a selective COX-2 inhibitor [18]. PGE₂ has been found to be a regulator of the number of hematopoietic stem cells in the zebrafish as well as to control proliferation and development of lymphocyte precursors and of oocyte maturation [41,45]. A role for leukotrienes has also been suggested by studies on mycobacterial infection showing increased susceptibility associated to the leukotriene A₄ hydrolase locus [43,46], and on traumatic brain injury showing a role for cysteinyl leukotriene signaling on neuronal regeneration [47]. Kidney marrow cells stimulated *in vitro* are able to synthesize

PGE₂, LTB₄, 5-HETE and 12-HETE from endogenous pools, presumably arachidonoyl-containing phospholipids. The profile of eicosanoids produced is similar to the ones observed in human and mouse neutrophils, although human neutrophils do not synthesize detectable amounts of PGE₂. Both human and mouse neutrophil preparations display some production of TXB₂ and LTC₄, possibly because of some contamination with platelets and eosinophils [23,24]. Zebrafish kidney marrow myeloid cells can also synthesize small amounts of LTB₅, a 5-LO product of EPA. LTB₅ contains an additional 17-*cis* double bond and shows 3–10 % chemotactic activity towards human neutrophils compared to LTB₄ [48]. It is somewhat surprising that in these cells, despite abundant levels of DHA-containing phospholipids and of free DHA, we could not detect any 17-OH-DHA, a known product of the oxidation of DHA and thought to be the precursor of resolvins and neuroprotectins, docosanoids involved in the resolution of the inflammatory process [3]. This is probably due to the fact that the release of eicosanoids in this model is driven by the initial activation of cPLA₂α and this enzyme shows remarkable selectivity for AA-containing phospholipids, while DHA-containing phospholipids are not good substrates [49].

While both COX and 5-LO products are detected in stimulated kidney marrow cells, it is remarkable that the most abundant eicosanoid found is 12-HETE, a product of 12-LO. This oxygenated metabolite of AA has been linked to a variety of biological activities and to pathologies such as cancer or cardiovascular disease [50,51]. Two isoforms of 12-LO are expressed in humans, 12*S*-LO expressed mainly in platelets, and 12*R*-LO expressed in skin [52,53]. Recent studies by two different groups have led to the identification of several zebrafish lipoxygenases [54,55], including an atypical 12*S*-LO which seems to be critical for normal embryonic development [55]. Another possible origin of 12-HETE could be from zebrafish cytochrome P450-catalyzed metabolism of AA. However, further characterization of the biosynthetic pathway leading to this metabolite was not examined and the role of 12-HETE in zebrafish remains to be investigated.

Analysis of the phospholipid composition of microsomes from zebrafish kidney marrow cells shows an abundance of molecular species containing polyunsaturated acyl chains, most prominently 22:6, but also 20:4 and 20:5. This is consistent with several reports on acyl composition of zebrafish larvae and adults [17,40,56,57]. Most of these studies were based on analyzing the acyl chain components of the different classes after hydrolyzing the phospholipid molecules. In this work we provide information about intact molecular species present in the zebrafish kidney marrow cell microsomes (Table 1). Many of the abundant phospholipids contain esterified 20:4, providing a plentiful endogenous pool for the synthesis of eicosanoids.

Previous studies conducted in our laboratory revealed that the organomercury compound thimerosal inhibited the two major arachidonoyl-CoA:lysophospholipid acyltransferases, MBOAT5 and MBOAT7, and greatly enhanced LTB₄ production in human neutrophils stimulated with GM-CSF and fMLP [23]. In a similar fashion, zebrafish kidney marrow cells exhibited a strong correlation between impaired ability to reincorporate free AA into phospholipids and increased synthesis of oxidized metabolites of AA. Although it shares some similarities, the spectrum of acyltransferase activities in microsomes from zebrafish kidney marrow cells differs in several respects from the spectrum in microsomes from

human neutrophils [15], particularly because 20:4-CoA seems to be a preferred substrate to reacylate most of the phospholipid classes. This probably contributes to the abundant presence of AA-containing phospholipids in these cells, especially in the case of PI where 20:4-containing molecular species are predominant. In contrast, the acyltransferase activities using 22:6-CoA, although readily measurable for PE and PC, cannot explain the abundance of 22:6-containing PA and PS. This is probably a consequence of both the high content of DHA in the diets commonly fed to zebrafish [17] and the expression and substrate preferences of many different enzymes involved in acyl chain exchange among phospholipid classes, including different phospholipases A₂, acyl-CoA synthases and CoA-independent transacylases. These possible contributions are yet to be investigated.

The results from the acyltransferase competitive assay suggested that zebrafish homologs of MBOAT5/LPCAT3, which reacylates PC, PS and PE, and MBOAT7/LPIAT1, which reacylates PI, are the major lysophospholipid acyltransferases present in this preparation. However, there was also clear evidence of the action of other acyltransferase activities, some of them not easily attributable to any of the known acyltransferases described so far. One instance is the robust incorporation of 18:0 chains into PI. This activity has also been observed in microsomes from human neutrophils and murine RAW 264.7 cells [28], suggesting that there are yet unknown acyltransferase activities that catalyze lysophospholipid reacylation.

In summary, a novel model of eicosanoid production in stimulated myeloid cells from zebrafish is presented in this manuscript. The most abundant phospholipid molecular species in zebrafish kidney marrow cells, many of them containing esterified 20:4, have been identified. The lysophospholipid acyltransferase activities that are important checkpoints controlling the levels of AA available for eicosanoid biosynthesis were evaluated in the zebrafish kidney marrow cells using a substrate competition assay.

Acknowledgments

We thank Dr. Angeles B. Ribera and Michelle Tellez from the Department of Physiology and Biophysics of the University of Colorado Denver for kindly providing larval and adult zebrafish and Dr. Joshua Black for providing expert advice on statistical analysis.

This work was supported by a grant from the National Institutes of Health (HL117798).

References

1. Haeggström JZ, Funk CD. Lipoxygenase and leukotriene pathways: biochemistry, biology, and roles in disease. *Chem Rev.* 2011; 111:5866–5898. [PubMed: 21936577]
2. Hirata T, Narumiya S. Prostanoids as regulators of innate and adaptive immunity. *Adv Immunol.* 2012; 116:143–174. [PubMed: 23063076]
3. Buckley CD, Gilroy DW, Serhan CN. Proresolving lipid mediators and mechanisms in the resolution of acute inflammation. *Immunity.* 2014; 40:315–327. [PubMed: 24656045]
4. Bergström S, Ryhage R, Samuelsson B, Sjövall J. The structure of prostaglandin E, F₁ and F₂. *Acta Chem Scand.* 1962; 16:501–502.
5. Murphy RC, Hammarström S, Samuelsson B. Leukotriene C: a slow-reacting substance from murine mastocytoma cells. *Proc Natl Acad Sci U S A.* 1979; 76:4275–4279. [PubMed: 41240]
6. Lands WEM. Metabolism of glycerolipids II. The enzymatic acylation of lysolecithin. *J Biol Chem.* 1960; 235:2233–2237. [PubMed: 14413818]

7. Ghosh M, Tucker DE, Burchett SA, Leslie CC. Properties of the Group IV phospholipase A₂ family. *Prog Lipid Res.* 2006; 45:487–510. [PubMed: 16814865]
8. Nomura DK, Morrison BE, Blankman JL, Long JZ, Kinsey SG, Marcondes MCG, Ward AM, Hahn YK, Lichtman AH, Conti B, Cravatt BF. Endocannabinoid hydrolysis generates brain prostaglandins that promote neuroinflammation. *Science.* 2011; 334:809–813. [PubMed: 22021672]
9. Chen X, Hyatt BA, Mucenski ML, Mason RJ, Shannon JM. Identification and characterization of a lysophosphatidylcholine acyltransferase in alveolar type II cells. *Proc Natl Acad Sci U S A.* 2006; 103:11724–11729. [PubMed: 16864775]
10. Nakanishi H, Shindou H, Hishikawa D, Harayama T, Ogasawara R, Suwabe A, Taguchi R, Shimizu T. Cloning and characterization of mouse lung-type acyl-CoA:lysophosphatidylcholine acyltransferase 1 (LPCAT1). Expression in alveolar type II cells and possible involvement in surfactant production. *J Biol Chem.* 2006; 281:20140–20147. [PubMed: 16704971]
11. Riekhof WR, Wu J, Jones JL, Voelker DR. Identification and characterization of the major lysophosphatidylethanolamine acyltransferase in *Saccharomyces cerevisiae*. *J Biol Chem.* 2007; 282:28344–28352. [PubMed: 17652094]
12. Shindou H, Hishikawa D, Nakanishi H, Harayama T, Ishii S, Taguchi R, Shimizu T. A single enzyme catalyzes both platelet-activating factor production and membrane biogenesis of inflammatory cells cloning and characterization of acetyl-CoA:lyso-PAF acetyltransferase. *J Biol Chem.* 2007; 282:6532–6539. [PubMed: 17182612]
13. Zhao Y, Chen YQ, Bonacci TM, Bredt DS, Li S, Bensch WR, Moller DE, Kowala M, Konrad RJ, Cao G. Identification and characterization of a major liver lysophosphatidylcholine acyltransferase. *J Biol Chem.* 2008; 283:8258–8265. [PubMed: 18195019]
14. Shindou H, Hishikawa D, Harayama T, Yuki K, Shimizu T. Recent progress on acyl CoA: lysophospholipid acyltransferase research. *J Lipid Res.* 2009; 50:S46–S51. [PubMed: 18931347]
15. Gijón MA, Riekhof WR, Zarini S, Murphy RC, Voelker DR. Lysophospholipid acyltransferases and arachidonate recycling in human neutrophils. *J Biol Chem.* 2008; 283:30235–30245. [PubMed: 18772128]
16. Pérez-Chacón G, Astudillo AM, Balgoma D, Balboa MA, Balsinde J. Control of free arachidonic acid levels by phospholipases A₂ and lysophospholipid acyltransferases. *Biochim Biophys Acta.* 2009; 1791:1103–1113. [PubMed: 19715771]
17. Almáida-Pagán PF, Lucas-Sánchez A, Tocher DR. Changes in mitochondrial membrane composition and oxidative status during rapid growth, maturation and aging in zebrafish, *Danio rerio*. *Biochim Biophys Acta.* 2014; 1841:1003–1011. [PubMed: 24769342]
18. Grosser T, Yusuff S, Cheskis E, Pack MA, FitzGerald GA. Developmental expression of functional cyclooxygenases in zebrafish. *Proc Natl Acad Sci U S A.* 2002; 99:8418–8423. [PubMed: 12011329]
19. Renshaw SA, Loynes CA, Elworthy S, Ingham PW, Whyte MKB. Modeling inflammation in the zebrafish: how a fish can help us understand lung disease. *Exp Lung Res.* 2007; 33:549–554. [PubMed: 18075830]
20. Wittmann C, Reischl M, Shah AH, Mikut R, Liebel U, Grabher C. Facilitating drug discovery: an automated high-content inflammation assay in zebrafish. *J Vis Exp.* 2012; 65:e4203. [PubMed: 22825322]
21. Yang LL, Wang GQ, Yang LM, Huang ZB, Zhang WQ, Yu LZ. Endotoxin molecule lipopolysaccharide-induced zebrafish inflammation model: a novel screening method for anti-inflammatory drugs. *Molecules.* 2014; 19:2390–2409. [PubMed: 24566310]
22. Thisse C, Thisse B. High-resolution in situ hybridization to whole-mount zebrafish embryos. *Nat Protoc.* 2008; 3:59–69. [PubMed: 18193022]
23. Zarini S, Gijón MA, Folco G, Murphy RC. Effect of arachidonic acid reacylation on leukotriene biosynthesis in human neutrophils stimulated with granulocyte-macrophage colony-stimulating factor and formyl-methionyl-leucyl-phenylalanine. *J Biol Chem.* 2006; 281:10134–10142. [PubMed: 16495221]
24. Gijón MA, Zarini S, Murphy RC. Biosynthesis of eicosanoids and transcellular metabolism of leukotrienes in murine bone marrow cells. *J Lipid Res.* 2006; 48:716–725. [PubMed: 17179116]

25. Bennett CM, Kanki JP, Rhodes J, Liu TX, Paw BH, Kieran MW, Langenau DM, Delahaye-Brown A, Zon LI, Fleming MD, Look AT. Myelopoiesis in the zebrafish, *Danio rerio*. *Blood*. 2001; 98:643–651. [PubMed: 11468162]
26. Westerfield, M. A guide for the laboratory use of zebrafish *Danio (Brachidanio) rerio*. Eugene: University of Oregon Press; 1995. The zebrafish book.
27. LeBlanc J, Bowman TV, Zon L. Transplantation of whole kidney marrow in adult zebrafish. *J Vis Exp*. 2007; 2:159. [PubMed: 18830422]
28. Martin SA, Gijón MA, Voelker DR, Murphy RC. Measurement of lysophospholipid acyltransferase activities using substrate competition. *J Lipid Res*. 2014; 55:782–791. [PubMed: 24563510]
29. Bligh EG, Dyer WJ. A rapid method of total lipid extraction and purification. *Can J Biochem Physiol*. 1959; 37:911–917. [PubMed: 13671378]
30. Steinhauer J, Gijón MA, Riekhof WR, Voelker DR, Murphy RC, Treisman JE. *Drosophila* lysophospholipid acyltransferases are specifically required for germ cell development. *Mol Biol Cell*. 2009; 20:5224–5235. [PubMed: 19864461]
31. Berry KA, Li B, Reynolds SD, Barkley RM, Gijón MA, Hankin JA, Henson PM, Murphy RC. MALDI imaging MS of phospholipids in the mouse lung. *J Lipid Res*. 2011; 52:1551–1560. [PubMed: 21508254]
32. Hall LM, Murphy RC. Electrospray mass spectrometric analysis of 5-hydroperoxy and 5-hydroxyeicosatetraenoic acids generated by lipid peroxidation of red blood cell ghost phospholipids. *J Am Soc Mass Spectrom*. 1998; 9:527–532. [PubMed: 9879367]
33. Liebisch G, Vizcaíno JA, Köfeler H, Trötz Müller M, Griffiths WJ, Schmitz G, Spener F, Wakelam MJ. Shorthand notation for lipid structures derived from mass spectrometry. *J Lipid Res*. 2013; 54:1523–1530. [PubMed: 23549332]
34. Morgan LT, Thomas CP, Kühn H, O'Donnell VB. Thrombin-activated human platelets acutely generate oxidized docosahexaenoic-acid-containing phospholipids via 12-lipoxygenase. *Biochem J*. 2010; 431:141–148. [PubMed: 20653566]
35. Dubyak GR, El-Moatassim C. Signal transduction via P₂-purinergic receptors for extracellular ATP and other nucleotides. *Am J Physiol*. 1993; 265:C577–C606. [PubMed: 8214015]
36. Axelsen PH, Murphy RC. Quantitative analysis of phospholipids containing arachidonate and docosahexaenoate chains in microdissected regions of mouse brain. *J Lipid Res*. 2010; 51:660–671. [PubMed: 19767534]
37. Martin CS, Moriyama A, Zon LI. Hematopoietic stem cells, hematopoiesis and disease: lessons from the zebrafish model. *Genome Med*. 2011; 3:83–93. [PubMed: 22206610]
38. Mione M, Meijer AH, Snaar-Jagalska BE, Spaink HP, Trede NS. Disease modeling in zebrafish: cancer and immune responses - a report on a workshop held in Spoleto, Italy, July 20–22, 2009. *Zebrafish*. 2009; 6:445–451. [PubMed: 20047471]
39. Henry KM, Loynes CA, Whyte MKB, Renshaw SA. Zebrafish as a model for the study of neutrophil biology. *J Leukoc Biol*. 2013; 94:633–642. [PubMed: 23463724]
40. Ho SY, Thorpe JL, Deng Y, Santana E, DeRose RA, Farber SA. Lipid metabolism in zebrafish. *Methods Cell Biol*. 2004; 76:87–108. [PubMed: 15602873]
41. Lister AL, Van Der Kraak G. An investigation into the role of prostaglandins in zebrafish oocyte maturation and ovulation. *Gen Comp Endocrinol*. 2008; 159:46–57. [PubMed: 18722378]
42. Yeh HC, Wang LH. Profiling of prostanoids in zebrafish embryonic development. *Prostaglandins Leukot Essent Fatty Acids*. 2006; 75:397–402. [PubMed: 17000094]
43. Tobin DM, Roca FJ, Oh SF, McFarland R, Vickery TW, Ray JP, Ko DC, Zou Y, Bang ND, Chau TT, Vary JC, Hawn TR, Dunstan SJ, Farrar JJ, Thwaites GE, King MC, Serhan CN, Ramakrishnan L. Host genotype-specific therapies can optimize the inflammatory response to mycobacterial infections. *Cell*. 2012; 148:434–446. [PubMed: 22304914]
44. Lebold KM, Kirkwood JS, Taylor AW, Choi J, Barton CL, Miller GW, Du JL, Jump DB, Stevens JF, Tanguay RL, Traber MG. Novel liquid chromatography-mass spectrometry method shows that vitamin E deficiency depletes arachidonic and docosahexaenoic acids in zebrafish (*Danio rerio*) embryos. *Redox Biol*. 2013; 2:105–113. [PubMed: 24416717]

45. Villablanca EJ, Pistocchi A, Court FA, Cotelli F, Bordignon C, Allende ML, Traversari C, Russo V. Abrogation of prostaglandin E₂/EP4 signaling impairs the development of *rag1*⁺ lymphoid precursors in the thymus of zebrafish embryos. *J Immunol*. 2007; 179:357–364. [PubMed: 17579056]
46. Scanga CA, Flynn JL. Mycobacterial infections and the inflammatory seesaw. *Cell Host Microbe*. 2010; 7:177–179. [PubMed: 20227659]
47. Kyritsis N, Kizil C, Zocher S, Kroehne V, Kaslin J, Freudenreich D, Iltzsche A, Brand M. Acute inflammation initiates the regenerative response in the adult zebrafish brain. *Science*. 2012; 338:1353–1356. [PubMed: 23138980]
48. Goldman DW, Pickett WC, Goetzl EJ. Human neutrophil chemotactic and degranulating activities of leukotriene B₅ (LTB₅) derived from eicosapentaenoic acid. *Biochem Biophys Res Commun*. 1983; 117:282–288. [PubMed: 6318749]
49. Shikano M, Masuzawa Y, Yazawa K, Takayama K, Kudo I, Inoue K. Complete discrimination of docosahexaenoate from arachidonate by 85 kDa cytosolic phospholipase A₂ during the hydrolysis of diacyl- and alkenylacylglycerophosphoethanolamine. *Biochim Biophys Acta*. 1994; 1212:211–216. [PubMed: 8180247]
50. Yeung J, Holinstat M. 12-Lipoxygenase: a potential target for novel anti-platelet therapeutics. *Cardiovasc Hematol Agents Med Chem*. 2011; 9:154–164. [PubMed: 21838667]
51. Porro B, Songia P, Squellerio I, Tremoli E, Cavalca V. Analysis, physiological and clinical significance of 12-HETE: a neglected platelet-derived 12-lipoxygenase product. *J Chromatogr B Analyt Technol Biomed Life Sci*. 2014; 964:26–40.
52. Yoshimoto T, Takahashi Y. Arachidonate 12-lipoxygenases. *Prostaglandins Other Lipid Mediat*. 2002; 68–69:245–262.
53. Boeglin WE, Kim RB, Brash AR. A 12R-lipoxygenase in human skin: mechanistic evidence, molecular cloning, and expression. *Proc Natl Acad Sci U S A*. 1998; 95:6744–6749. [PubMed: 9618483]
54. Jansen C, Hofheinz K, Vogel R, Roffeis J, Anton M, Reddanna P, Kuhn H, Walther M. Stereocontrol of arachidonic acid oxygenation by vertebrate lipoxygenases. Newly cloned zebrafish lipoxygenase 1 does not follow the Ala-versus-Gly concept. *J Biol Chem*. 2011; 286:37804–37812. [PubMed: 21880725]
55. Haas U, Raschperger E, Hamberg M, Samuelsson B, Tryggvason K, Haeggström JZ. Targeted knock-down of a structurally atypical zebrafish 12S-lipoxygenase leads to severe impairment of embryonic development. *Proc Natl Acad Sci*. 2011; 108:20479–20484. [PubMed: 22143766]
56. Ong ES, Chor CF, Zou L, Ong CN. A multi-analytical approach for metabolomic profiling of zebrafish (*Danio rerio*) livers. *Mol Biosyst*. 2009; 5:288–298. [PubMed: 19225620]
57. Miyares RL, de Rezende VB, Farber SA. Zebrafish yolk lipid processing: a tractable tool for the study of vertebrate lipid transport and metabolism. *Dis Model Mech*. 2014; 7:915–927. [PubMed: 24812437]

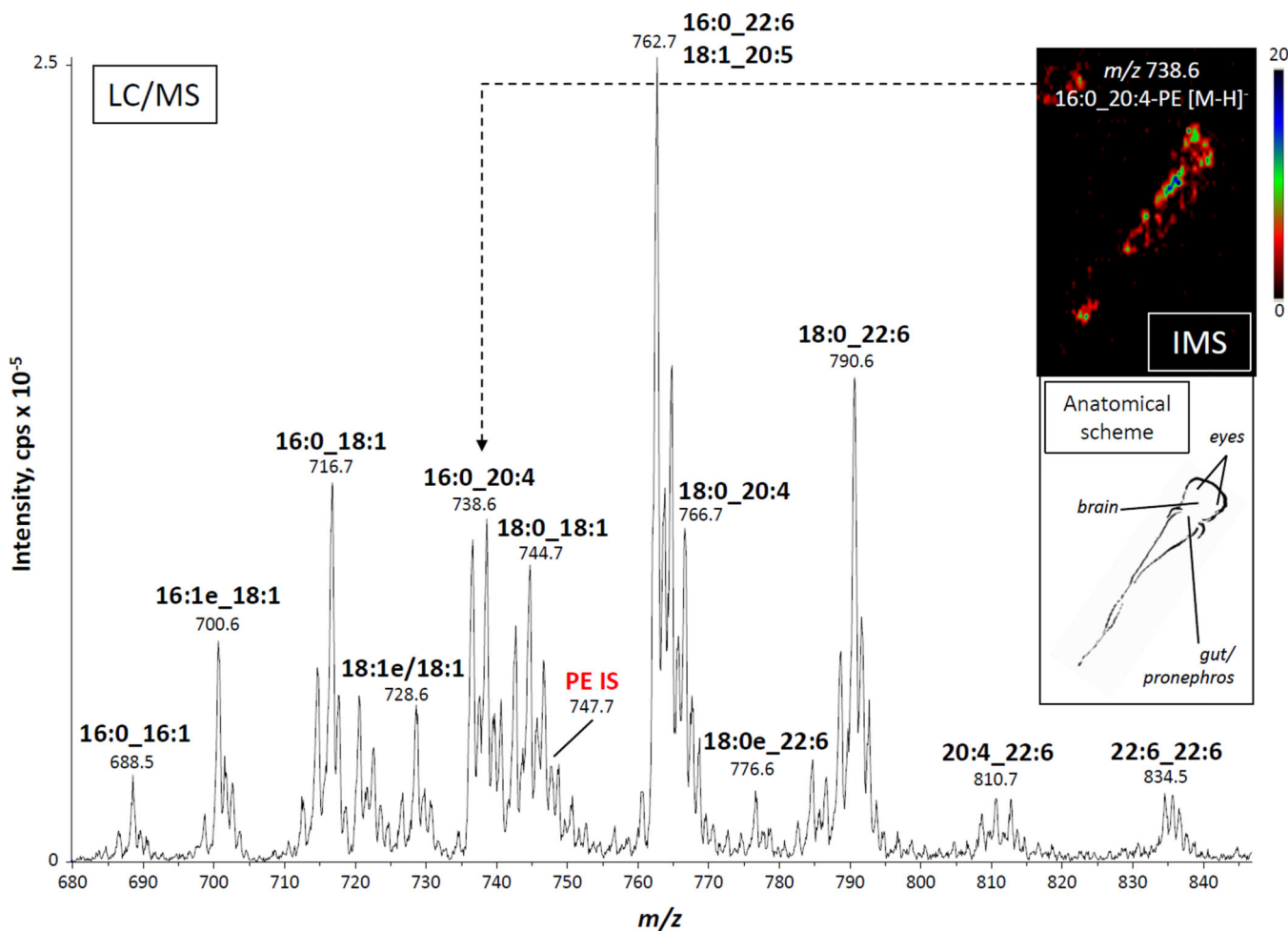


Fig. 1.

Electrospray mass spectrum of phosphatidylethanolamines in an adult zebrafish kidney and mass spectral image of the distribution of $16:0_{-}20:4$ -PE in larval zebrafish. LC-MS analysis of PEs from an extract of whole zebrafish kidney homogenate. IS: internal standard, [$^2\text{H}_3$] $16:0/18:1$ -PE. Inset: 10- μm thick slice from a 3 dpf zebrafish analyzed by MALDI-TOF-based imaging mass spectrometry (IMS). The image was generated by plotting the intensity of the m/z 738.6 ion ($16:0_{-}20:4$ -PE). An anatomical scheme based on a public-access atlas (www.zfin.org) is shown to indicate the approximate location of the IMS signal.

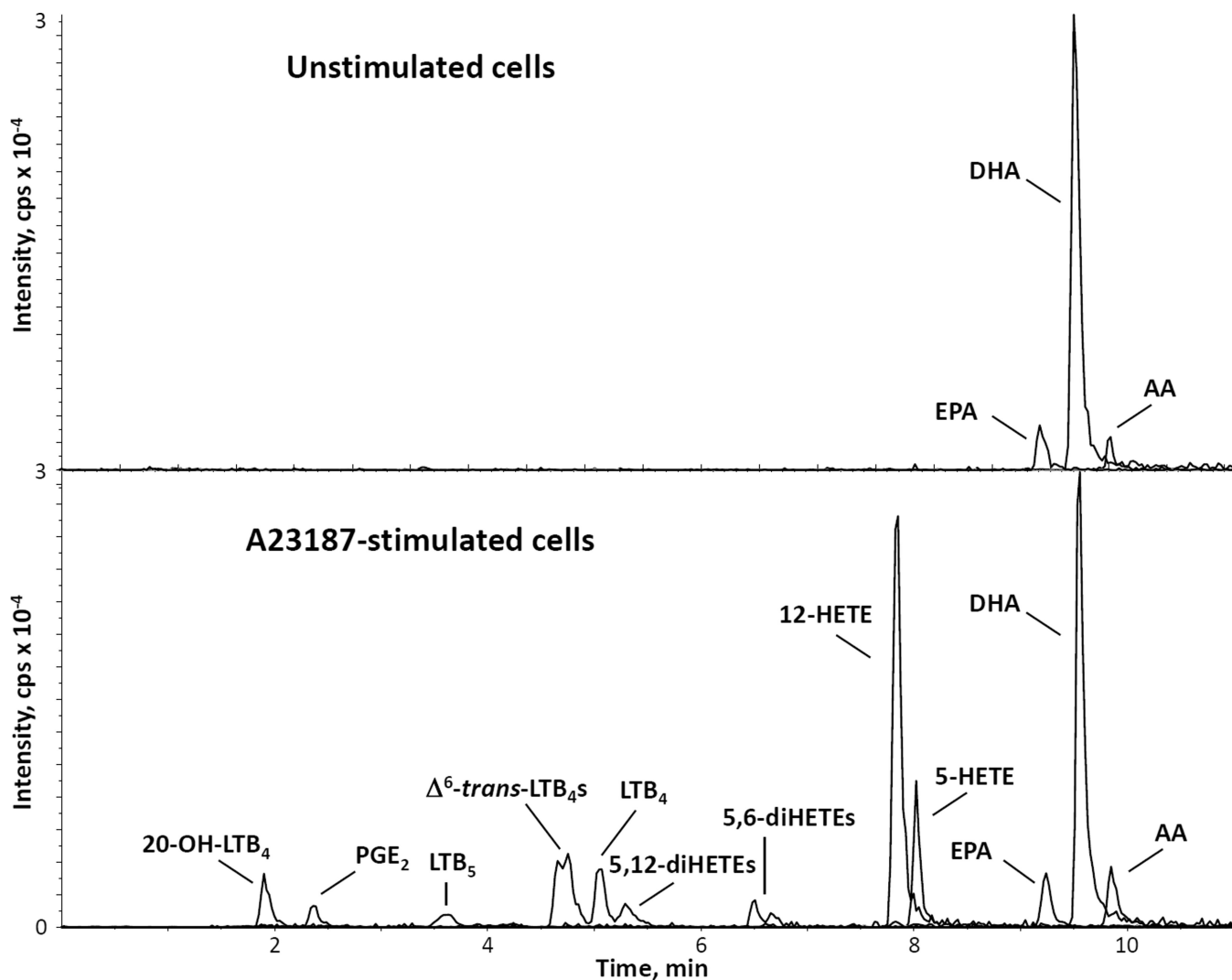


Fig. 2. LC-MS/MS profile of eicosanoid production in zebrafish kidney marrow cells. Cell extracts from kidney marrow cells (1×10^6), either unstimulated or stimulated with $0.5 \mu\text{M}$ calcium ionophore for 15 min at $28.5 \text{ }^\circ\text{C}$ were analyzed by reverse-phase liquid chromatography/tandem mass spectrometry. Mass spectrometric analysis was performed in the negative ion mode by multiple reaction monitoring of specific mass transitions corresponding to analytes and deuterated internal standards. The graphs show an overlay of the signals corresponding to the compounds indicated, and are representative of three experiments performed with different marrow cell preparations.

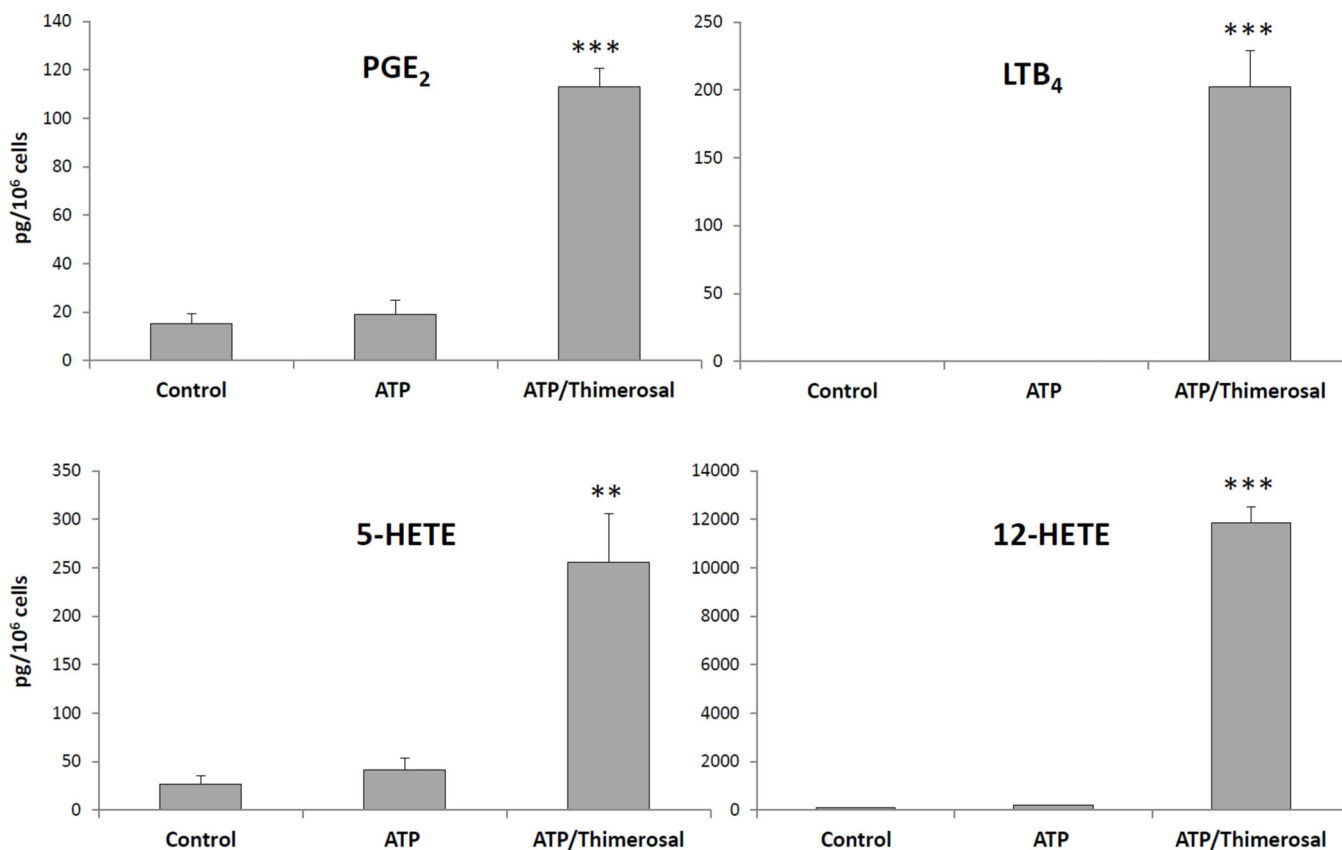


Fig. 3. Eicosanoid production in zebrafish kidney marrow cells stimulated with ATP: effect of thimerosal pretreatment. PGE₂, LTB₄, 5-HETE, and 12-HETE production in kidney marrow cells (1×10^6) stimulated at 28.5 °C with ATP (0.1 mM, 15 min) in the presence or absence of thimerosal (25 μ M). Control samples were left untreated. Eicosanoids were analyzed by LC-MS/MS in the MRM mode and quantitation was performed using standard isotope dilution. Results are expressed as average \pm SEM of at least 4 experiments. ** $p < 0.01$, *** $p < 0.001$, calculated using one-way ANOVA.

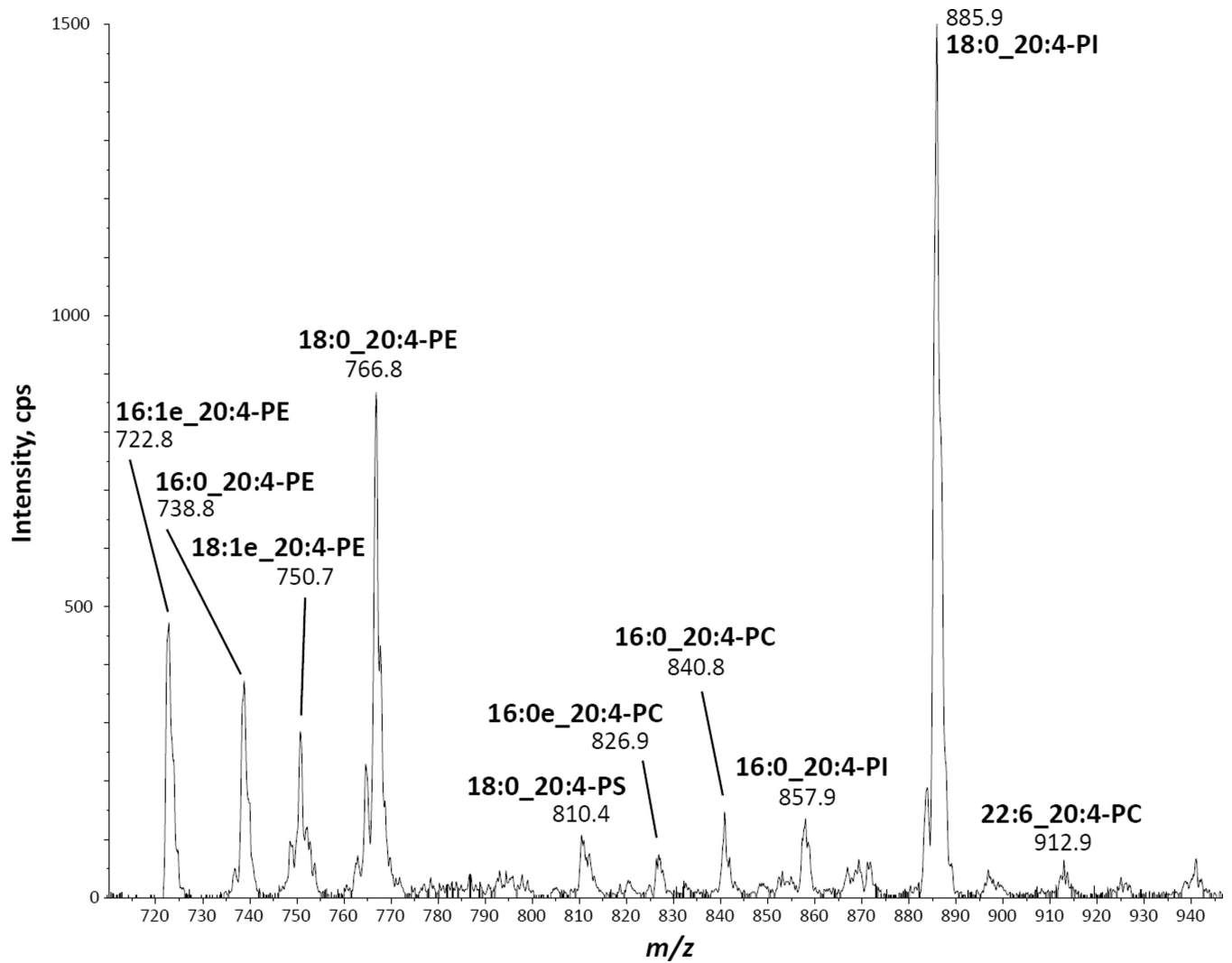


Fig. 4. LC-MS/MS analysis of AA-containing phospholipids in microsome extracts from zebrafish kidney marrow cells. Analysis was performed by normal phase HPLC followed by precursor ion scanning of the m/z 303 fragment, corresponding to the arachidonoyl carboxylate anion.

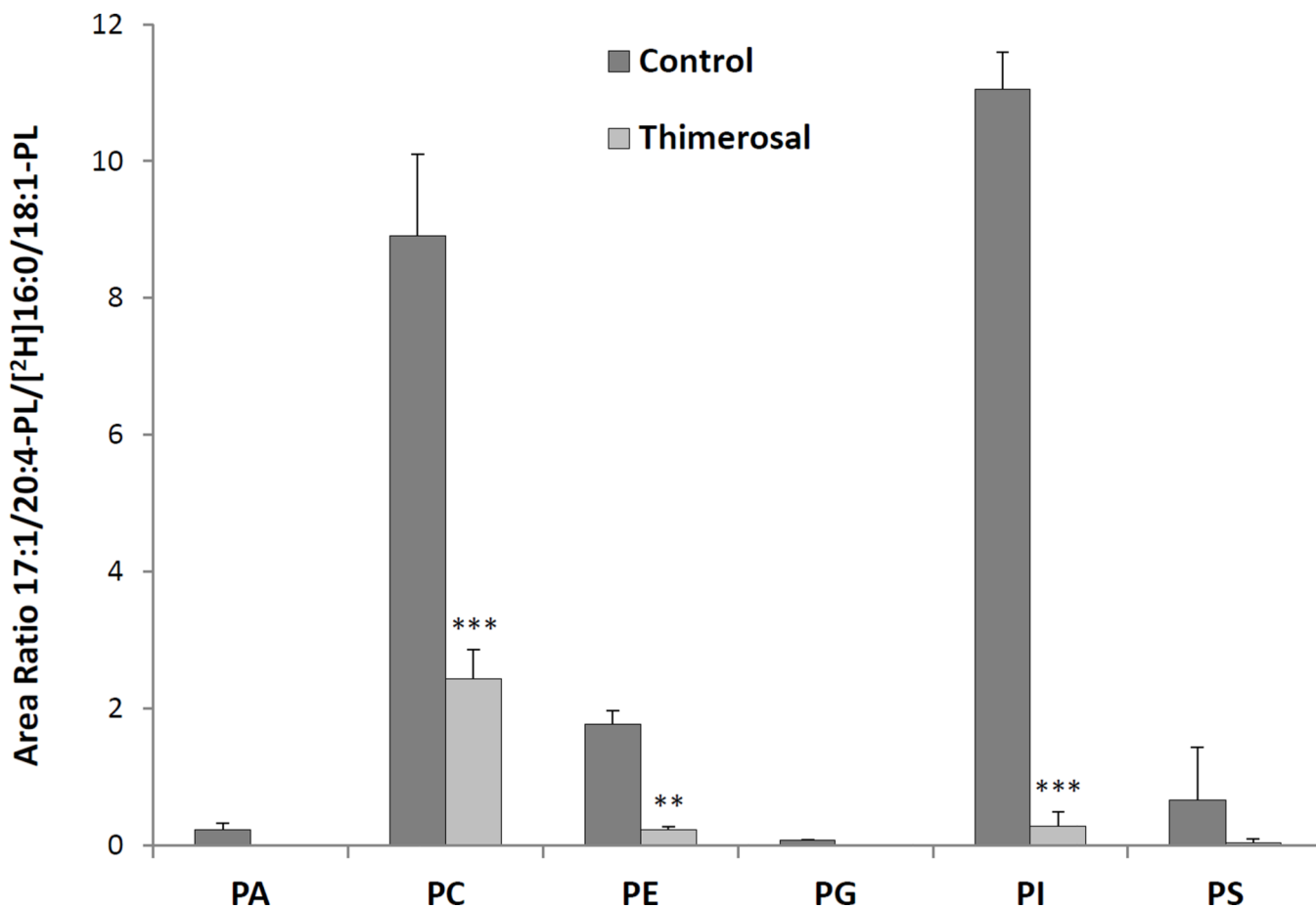


Fig. 5. Lysophospholipid:arachidonoyl-CoA acyltransferase activities in microsomes from zebrafish kidney marrow cells. Kidney marrow cell microsomes (10 μg protein) were incubated with 3 μM each of eight different acyl-CoAs and 3 μM each of six lysophospholipids, in the presence or absence of 50 μM thimerosal. Mass spectrometric analysis was performed in the negative ion mode using MRM, and results are reported as area ratio between analyte and corresponding deuterated internal standard. Results are expressed as average area ratio \pm SD of at least 3 experiments. ** $p < 0.01$, *** $p < 0.001$, calculated using repeated measures two-way ANOVA.

Table 1
Phospholipid molecular species in microsomes from zebrafish kidney marrow cells

Normal phase LC-MS/MS analysis was performed in the negative ion mode using scheduled MRM based on the combinations of the more common acyl chains. Results are shown as percentage of each individual species

relative to the most abundant species for each class. Cells in white represent molecular species below the limit of detection of this specific assay.

Molecular Species	PA	PC	PE	PG	PI	PS	Molecular Species	PA	PC	PE	PG	PI	PS
14:0_16:0							16:0e_16:0						
16:0_16:0							16:0e_16:1						
16:0_16:1							16:0e_18:0						
16:0_18:0							16:0e_18:1						
16:0_18:1							16:0e_18:2						
16:0_18:2							16:0e_18:3						
16:0_18:3							16:0e_20:4						
16:0_20:4							16:0e_20:5						
16:0_20:5							16:0e_22:6						
16:0_22:6							16:1e_16:0						
16:1_16:1							16:1e_16:1						
16:1_18:0							16:1e_18:1						
16:1_18:1							16:1e_18:2						
16:1_18:2							16:1e_18:3						
16:1_18:3							16:1e_20:4						
16:1_20:4							16:1e_20:5						
16:1_20:5							16:1e_22:6						
16:1_22:6							18:0e_16:0						
18:0_18:0							18:0e_16:1						
18:0_18:1							18:0e_18:0						
18:0_18:2							18:0e_18:1						
18:0_18:3							18:0e_18:2						
18:0_20:4							18:0e_20:4						
18:0_20:5							18:0e_20:5						
18:0_22:6							18:0e_22:6						
18:1_18:1							18:1e_16:0						
18:1_18:2							18:1e_16:1						
18:1_18:3							18:1e_18:0						
18:1_20:4							18:1e_18:1						
18:1_20:5							18:1e_18:2						
18:1_22:6							18:1e_18:3						
18:2_18:2							18:1e_20:4						
18:2_18:3							18:1e_20:5						
18:2_20:4							18:1e_22:6						
18:2_20:5							% of Most Abundant Species within Class						
18:2_22:6							ND						
20:4_20:4							0.1 - 5						
20:4_20:5							5 - 20						
20:4_22:6							20 - 50						
20:5_22:6							50 - 99						
22:6_22:6							100						

Table 2
Lysophospholipid acyltransferase activities in microsomes from zebrafish kidney marrow cells

Kidney marrow cell microsomes (10 µg protein) were incubated with 3 µM each of eight different acyl-CoAs and six lysophospholipids. Normal phase LC-MS/MS analysis was performed in the negative ion mode using MRM of all the molecular species that can be potentially generated during the reaction, and results are reported as area ratio between analyte and corresponding deuterated internal standard. Results are expressed as average area ratio ± SD of at least 3 experiments. Area ratios below 1 %, which showed very low signal-to-noise ratios, were considered to be below the detection limit (not detected, ND).

	Acyl-CoA	Area Ratio	Acyl-CoA	Area Ratio
Lyso-PA	14:0	0.06 ± 0.01	14:0	0.02 ± 0.00
	16:0	0.11 ± 0.02	16:0	0.03 ± 0.01
	18:0	0.09 ± 0.03	18:0	0.14 ± 0.01
	18:1	0.05 ± 0.03	18:1	0.03 ± 0.01
	18:2	ND	18:2	0.02 ± 0.01
	20:4	0.23 ± 0.09	20:4	0.07 ± 0.01
	20:5	ND	20:5	0.01 ± 0.01
	22:6	ND	22:6	ND
Lyso-PC	14:0	7.16 ± 1.37	14:0	ND
	16:0	7.41 ± 1.73	16:0	0.43 ± 0.10
	18:0	2.75 ± 0.80	18:0	1.98 ± 0.12
	18:1	3.28 ± 0.73	18:1	0.50 ± 0.08
	18:2	2.31 ± 0.56	18:2	0.03 ± 0.03
	20:4	8.91 ± 1.19	20:4	11.06 ± 0.53
	20:5	8.55 ± 1.85	20:5	0.47 ± 0.03
	22:6	3.92 ± 0.86	22:6	ND
Lyso-PE	14:0	0.12 ± 0.01	14:0	ND
	16:0	0.73 ± 0.04	16:0	0.07 ± 0.01
	18:0	4.39 ± 0.14	18:0	0.48 ± 0.03
	18:1	0.48 ± 0.02	18:1	ND
	18:2	0.22 ± 0.03	18:2	0.04 ± 0.02
	20:4	1.77 ± 0.19	20:4	0.66 ± 0.77
Lyso-PG				
Lyso-PI				
Lyso-PS				

	Acyl-CoA	Area Ratio	Acyl-CoA	Area Ratio
	20:5	1.00 ± 0.09	20:5	0.83 ± 0.17
	22:6	0.72 ± 0.05	22:6	0.14 ± 0.07